A library of stellar light variations due to extra-solar comets

A. Lecavelier des Etangs[1]

Institut d'Astrophysique de Paris, CNRS, 98bis Boulevard Arago, F-75014 Paris, France

Abstract. We present an extensive study of stellar occultations by extra-solar cometary tails through a large number of numerical simulations. The output of the simulations are the star light extinction and scattering as a function of time at three wavelengths (400, 800 and 2200 nm). We explore the light curves dependence over a large set of possible parameters (dust size distributions, stellar types, production rates, orbital configurations). This grid of models, which is electronically available at http://www.iap.fr/users/lecaveli/grid/, will be useful to develop and to test the detection methods, and to analyze the results of the forthcoming high accuracy photometric surveys.

With this tool, we quantify the proportion of light curves which could mimic a planetary occultation. We find that at a signal to noise ratio of 10, about 5% of cometary occultation light curves are symmetric enough to be mistaken for a planetary occultation. The total number of planet mimicing cometary occultations could be of the same order as the number of planet occultations.

Key words: methods: numerical — occultations — comets: general — planetary systems

1. Introduction

In a previous paper, we have shown the important possibility of detecting extra-solar cometary activity from a photometric survey (Lecavelier des Etangs et al. 1999, hereafter LVF 99). Taking the COROT space mission as an example, we consider that a survey of several tens of thousands of stars with a photometric accuracy of $\sim 10^{-4}$ during several months will be achievable in the very near future (Baglin et al. 1997).

We have shown that the occultation of a star by an orbiting extra-solar comet can result in a photometric variation of the star. In most cases the light curve shows a

Send offprint requests to: A. Lecavelier des Etangs

very peculiar "rounded triangular" shape; but some light curves can mimic planetary occultation. With only a small number of simulations available, it was not possible to accurately determine the proportion of light curves which mimic the planetary occultation.

We also gave the probabilities of detecting comets using a large photometric survey. We found that by the observation of several tens of thousands of stars, it should be possible to detect several hundreds of occultations per year. This last number is larger than the number of expected planetary occultations by Jupiter-like planets, making the cometary occultations a powerful tool to look into the planetary systems' structure and evolution.

However, due to the large computer-time needed by the simulations, only a small set of parameters had been investigated. To better analyze the observations and to determine the specific effects of the parameters, a wide range of input parameters must be considered. We thus decided to compute a large grid of stellar light variations due to the cometary occultations and make the results widely available through an electronic access on the web server http://www.iap.fr/users/lecaveli/grid/

The aim of this work is to provide a large database of simulated cometary occultations which can be used to develop the reduction methods for the photometric surveys and can help for the analysis of future observational results. To accomplish this task, we used the model and code presented in Lecavelier des Etangs et al. (1999) (LVF 99). The database is presented in the form of a list of files. Each file corresponds to different values of the parameters. Six parameters are needed to define the position in the grid: the dust size distribution, the type of the central star, the dust production rate, the periastron distance, the longitude of the periastron, and the inclination of the comet orbit. Each file gives the extinction and scattering of the star light by the cometary cloud as a function of time at three wavelengths: 400 (B), 800 (R) and 2200 nm (K).

In Sect. 2, we describe the model parameters needed to define a cometary occultation. Examples of expected light

curves are given in Sect. 3. Estimates of the proportion of light curves which could be mistaken as due to planetary occultation are given in Sect. 4. The conclusion is in Sect. 5.

2. Input parameters

2.1. Size distribution

Because the sensitivity to radiation pressure depends on the particle size, the size distribution is an important parameter which determines the geometry of the comet dust cloud. As in LVF 99, we assume a size distribution $dn(s)$ of the form

$$dn(s) = \frac{(1 - s_0/s)^m}{s^n}. \tag{1}$$

where s is the dust size. Here we used three different dust size distributions. The distribution used in LVF 99 is defined by $s_0 = 0.1$ μm, $n = 4.2$, $m = n(s_p - s_0)/s_0$, and $s_p = 0.50$ μm (Hanner 1983; Newburn & Spinrad 1985). Following the value of the peak s_p, this distribution is named "50".

Two other distributions have been used and correspond to distributions observed at small distances from the Sun ($\lesssim 0.5$ AU). These distributions are peaked at smaller sizes (Newburn & Spinrad 1985). The larger quantity of small dust particles increases the chromatic signature of the light variation. The distribution named "20" has the following parameters $s_0 = 0.05$ μm, $n = 4.2$, and $s_p = 0.20$ μm. The distribution named "25" is an intermediate distribution with $s_0 = 0.1$ μm, $n = 4.2$, and $s_p = 0.25$ μm.

As in LVF 99, we consider the β ratio of the radiation force to the gravitational force to be

$$\beta = 0.2 \left(\frac{L_*/M_*}{L_\odot/M_\odot} \right) \left(\frac{s}{1\ \mu m} \right)^{-1} \tag{2}$$

where L_*/M_* is the luminosity-mass ratio of the central star.

2.2. Stellar parameters

The simulations depend on the mass, luminosity and radius of the central star (M_*, L_* and R_*). We have chosen to use five sets of parameters for the star, each set corresponding to a given type of star: M0V, K0V, G0V, F0V or A0V (Table 1).

2.3. Production rate

The production rate is the main parameter which determines the amplitude of the photometric variation. The dust production rate P is assumed to vary with L_*, the

Table 1. The five triplets of mass, radius and luminosity/mass ratio used for the central star

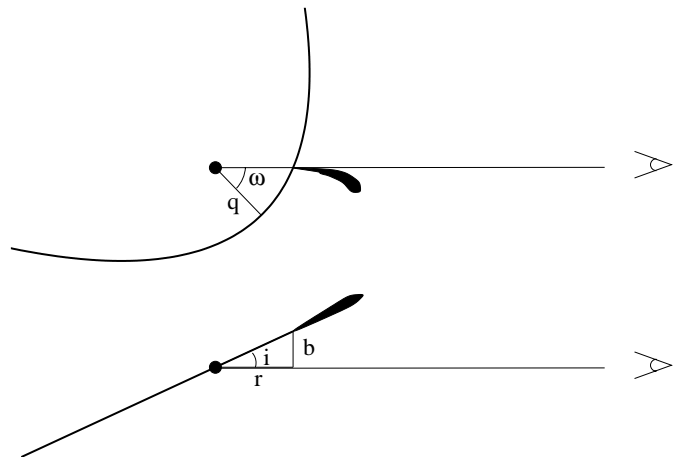| Type	Mass $(M_\odot)$	Radius $(R_\odot)$	Luminosity/Mass $(L_\odot/M_\odot)$
M0V	0.5	0.63	0.13
K0V	0.7	0.85	0.50
G0V	1.1	1.05	1.15
F0V	1.7	1.35	3.70
A0V	3.2	2.50	25.00

Fig. 1. Sketch of the orbital configuration and description of the orbital parameters

luminosity of the star and r, the distance to the star. P is taken to be

$$P = P_0 \left(\frac{r}{r_0} \right)^{-2} \left(\frac{L_*}{L_\odot} \right) \tag{3}$$

(see, for instance, Schleicher et al. 1998). P_0, the rate at a characteristic distance $r_0 = 1$ AU and for a solar luminosity is an input parameter. We used five different values with $\log(P_0/\mathrm{kg\ s}^{-1}) = 2, 3, 4, 5, 6$. The dust production is taken to be zero beyond a critical distance $r_{\mathrm{crit.}} = 3\sqrt{L_*/L_\odot}$ AU (Biver et al. 1997).

2.4. Orbital parameters

Finally, as already seen in LVF 99, the orbital characteristics of the comet define the shape of the light curve. We only considered comets on parabolic orbits (Fig. 1).

2.4.1. Periastron

The periastron distance q is obviously an important parameter. Changing its value changes the time scale of the variation and the amplitude through the production rate (Eq. 3). We set the periastron to six different values ranging from 0.3 AU to 2.0 AU: (0.3; 0.5; 0.7; 1.0; 1.5; 2.0).

Table 2. Naming convention for the models as a function of the parameters value. Each column gives the corresponding naming-substring for each parameter. The final name is obtained by the concatenation of the naming sub-strings and separated by underscores. For instance, with a size distribution with $s_p = 0.25$ μm, a central star of F type, a production rate of 10^4 kg s^{-1} (at $r_0 = 1$ AU), a periastron at 0.5 AU and at 45 degrees from the line of sight, and an impact parameter $b = 0.33$ R_*, the model-name is "25_F_40_05_p2_03" and the corresponding filename in the database is "flux_25_F_40_05_p2_03"

Size distribution	name	Stellar type name	Production (kg s^{-1})	name	Periastron (AU)	name	ω (°)	name	(°)	name	Impact parameter (R_*)	name
$s_p = 0.20$ μm	20	M	10^2	20	0.3	03	−157.5	m7	157.5	p7	0	00
$s_0 = 0.05$ μm, $n = 4.2$		K	10^3	30	0.5	05	−135.0	m6	135.0	p6	0.33	03
		G	10^4	40	0.7	07	−112.5	m5	112.5	p5	0.66	06
$s_p = 0.25$ μm	25	F	10^5	50	1.0	10	−90.0	m4	90.0	p4	1.00	10
$s_0 = 0.1$ μm, $n = 4.2$		A	10^6	60	1.5	15	−67.5	m3	67.5	p3	1.33	13
					2.0	20	−45.0	m2	45.0	p2	1.66	16
$s_p = 0.50$ μm	50						−22.5	m1	22.5	p1		
$s_0 = 0.1$ μm, $n = 4.2$							0.0	00				

Table 3. Example of an 8-columns table from the file corresponding to the model "50_G_50_10_00_00"

t	E	E_b	E_r	E_k	$F\mathrm{sca}_b$	$F\mathrm{sca}_r$	$F\mathrm{sca}_k$
−0.63	0.000E+00	0.000E+00	0.000E+00	0.000E+00	0.136E-06	0.878E-07	0.595E-07
−0.56	0.000E+00	0.000E+00	0.000E+00	0.000E+00	0.152E-06	0.101E-06	0.668E-07
−0.50	0.000E+00	0.000E+00	0.000E+00	0.000E+00	0.172E-06	0.119E-06	0.750E-07
−0.44	0.000E+00	0.000E+00	0.000E+00	0.000E+00	0.200E-06	0.149E-06	0.839E-07
−0.38	0.000E+00	0.000E+00	0.000E+00	0.000E+00	0.240E-06	0.196E-06	0.932E-07
−0.31	0.000E+00	0.000E+00	0.000E+00	0.000E+00	0.317E-06	0.264E-06	0.103E-06
−0.25	0.000E+00	0.000E+00	0.000E+00	0.000E+00	0.485E-06	0.356E-06	0.113E-06
−0.19	−0.795E-05	−0.795E-05	−0.795E-05	−0.647E-05	0.770E-06	0.470E-06	0.123E-06
−0.13	−0.304E-04	−0.304E-04	−0.301E-04	−0.240E-04	0.112E-05	0.587E-06	0.133E-06
−0.06	−0.383E-04	−0.383E-04	−0.374E-04	−0.306E-04	0.140E-05	0.689E-06	0.145E-06
0.00	−0.404E-04	−0.404E-04	−0.395E-04	−0.322E-04	0.157E-05	0.758E-06	0.157E-06
0.06	−0.413E-04	−0.413E-04	−0.404E-04	−0.325E-04	0.159E-05	0.771E-06	0.168E-06
0.13	−0.417E-04	−0.417E-04	−0.408E-04	−0.328E-04	0.146E-05	0.728E-06	0.174E-06
0.19	−0.371E-04	−0.371E-04	−0.360E-04	−0.280E-04	0.119E-05	0.640E-06	0.174E-06
0.25	−0.210E-04	−0.210E-04	−0.202E-04	−0.145E-04	0.885E-06	0.530E-06	0.166E-06
0.31	−0.127E-04	−0.127E-04	−0.125E-04	−0.805E-05	0.666E-06	0.420E-06	0.150E-06
0.38	−0.122E-04	−0.122E-04	−0.120E-04	−0.797E-05	0.527E-06	0.322E-06	0.131E-06
0.44	−0.105E-04	−0.105E-04	−0.105E-04	−0.818E-05	0.461E-06	0.251E-06	0.111E-06
0.50	−0.866E-05	−0.866E-05	−0.866E-05	−0.699E-05	0.406E-06	0.203E-06	0.936E-07
0.56	−0.754E-05	−0.754E-05	−0.754E-05	−0.512E-05	0.379E-06	0.176E-06	0.794E-07
0.63	−0.824E-05	−0.824E-05	−0.824E-05	−0.582E-05	0.355E-06	0.161E-06	0.687E-07
0.69	−0.537E-05	−0.537E-05	−0.537E-05	−0.360E-05	0.333E-06	0.150E-06	0.606E-07
0.75	−0.474E-05	−0.474E-05	−0.474E-05	−0.333E-05	0.310E-06	0.141E-06	0.542E-07
0.81	−0.428E-05	−0.428E-05	−0.428E-05	−0.287E-05	0.287E-06	0.134E-06	0.488E-07
0.87	−0.352E-05	−0.352E-05	−0.352E-05	−0.211E-05	0.266E-06	0.127E-06	0.442E-07
0.94	−0.299E-05	−0.299E-05	−0.299E-05	−0.262E-05	0.248E-06	0.122E-06	0.440E-07
1.00	−0.173E-05	−0.173E-05	−0.173E-05	−0.169E-05	0.232E-06	0.116E-06	0.399E-07
1.06	−0.236E-05	−0.236E-05	−0.236E-05	−0.224E-05	0.220E-06	0.110E-06	0.364E-07
1.13	−0.324E-05	−0.324E-05	−0.324E-05	−0.275E-05	0.209E-06	0.105E-06	0.334E-07
1.19	−0.375E-05	−0.375E-05	−0.375E-05	−0.326E-05	0.200E-06	0.101E-06	0.308E-07
1.25	−0.485E-05	−0.485E-05	−0.454E-05	−0.372E-05	0.191E-06	0.963E-07	0.286E-07

2.4.2. Longitude of periastron

As shown in LVF 99, the symmetry of the light curve depends essentially on the longitude of the periastron ω. We sampled the longitude of the periastron from −157.5 degrees to +157.5 degrees from the line of sight by step of 22.5 degrees.

2.4.3. Inclination and impact parameter

Because there is an invariance against the rotation along the line of sight, we can consider that the ascending node is at 90 degrees from the line of sight. Thus, the inclination (i) is defined by the impact parameter of the orbit (b) projected on the sky.
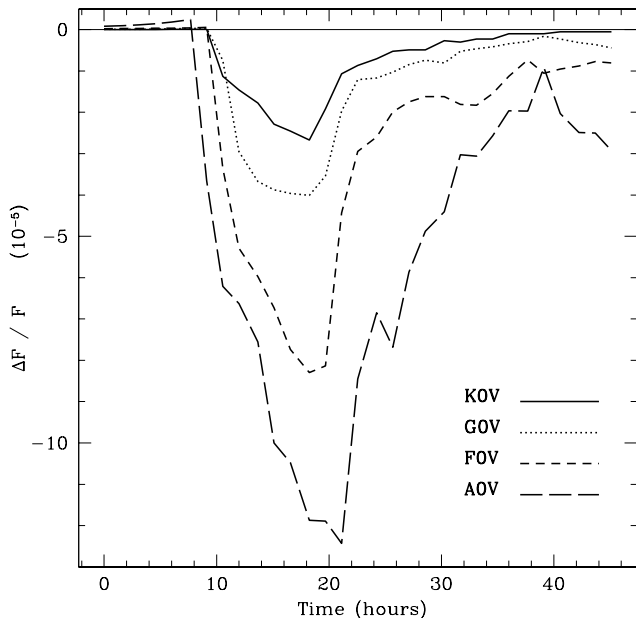
$$i = \tan^{-1}(b/r) \tag{4}$$

Fig. 2. Plot of the photometric variations during a cometary occultation observed in red ($\lambda = 8000$ Å). The variation is calculated by the addition of the star light scattering and extinction, both obtained from the models "50_K_50_10_00_00", "50_G_50_10_00_0", "50_F_50_10_00_00" and "50_A_50_10_00_00". The production rate is 10^5 kg s^{-1} at 1 AU for a solar luminosity. The comet orbit crosses the line of sight at the periastron $q = 1$ AU (longitude of periastron and impact parameter are zero). These light curves present the very specific "rounded triangular" shape observed in the majority of simulations of cometary occultations. The amplitude of the variation is proportional to the production rate and inversely proportional to β, the sensitivity to the radiation pressure which disperses the dust. As a result, at a given production rate P_0, the amplitude of the variation is roughly proportional to the mass of the central star

where r is the distance of the comet to the star when crossing the line of sight. The grid of model has been calculated with six different values of b: $b/R_* = 0.00, 0.33, 0.66, 1.00, 1.33, 1.66$. The corresponding models are named by two-character strings which are 00, 03, 06, 10, 13, 16 (Table 2).

3. Results

3.1. Naming convention

The parameter space is a 6-dimensional space (size distribution, stellar type, P_0, q, ω, b). For each parameter the range of value has been sampled at several positions. The number of positions for each parameter is (3, 5, 5, 6, 15, 6). In fact, comets at 2 AU from a K type star or farther than 0.7 AU from a M type star are beyond the water ices sublimation limit and should not evaporate. The models with $P_0 = 10^6$ kg s^{-1} have not been calculated for A stars
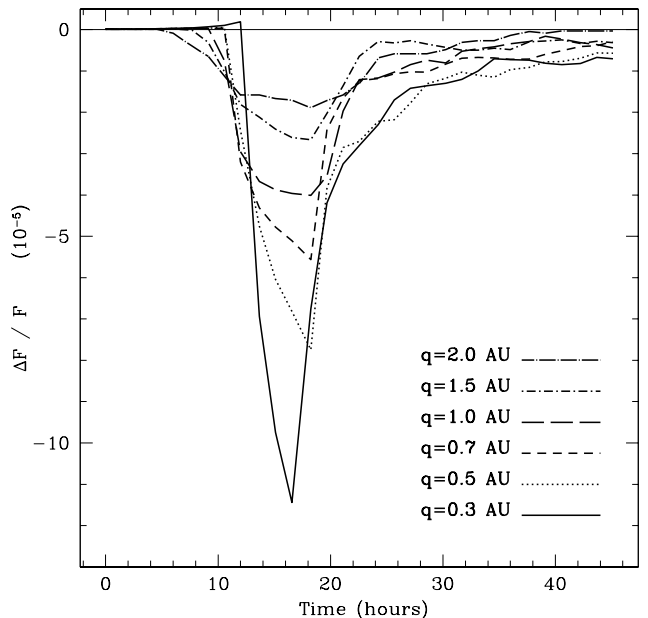
Fig. 3. Same as Fig. 2. Here all the parameters are the same except that the star is always taken to be a G type star and the periastron distance is allowed to vary form 0.3 AU to 2.0 AU. Of course, the amplitude of the variation significantly increases when the periastron decreases

because of computer-time limitation. Finally, we obtain 33480 different models for the M, K G, F, and A stars ($3 \times 5 \times 3 \times 15 \times 6 + 3 \times 5 \times 5 \times 15 \times 6 + 3 \times 5 \times 6 \times 15 \times 6 + 3 \times 5 \times 6 \times 15 \times 6 + 3 \times 4 \times 6 \times 15 \times 6$).

Each resulting model is given a name composed by the names of the parameters and underscores. For example, with the dust size distribution so-called "50", a comet orbiting a G type star with a production rate of 10^5 kg s^{-1} and a periastron at 1 AU located on the line of sight ($\omega = 0$, $b = 0$), the model-name is "50_G_50_10_00_00". The name-substrings corresponding to parameters values are given in Table 2.

3.2. Files content

Each file has an header giving the value of the parameters used in the simulation and an 8-columns table. This table gives the light variation as a function of the time during 45 hours with a time-step of 1.5 hours. The first column gives the time in days relative to the periastron passage. The second column gives the maximal fraction of the stellar light extinct by the comet dust cloud. This maximal extinction is obtained by considering a wavelength of observation shorter than the size of any dust particle. The Cols. 3 to 5 give the fraction of the stellar light extinct by the comet at wavelengths 400, 800 and 2200 nm, roughly corresponding to observations in the B, R and K bands.
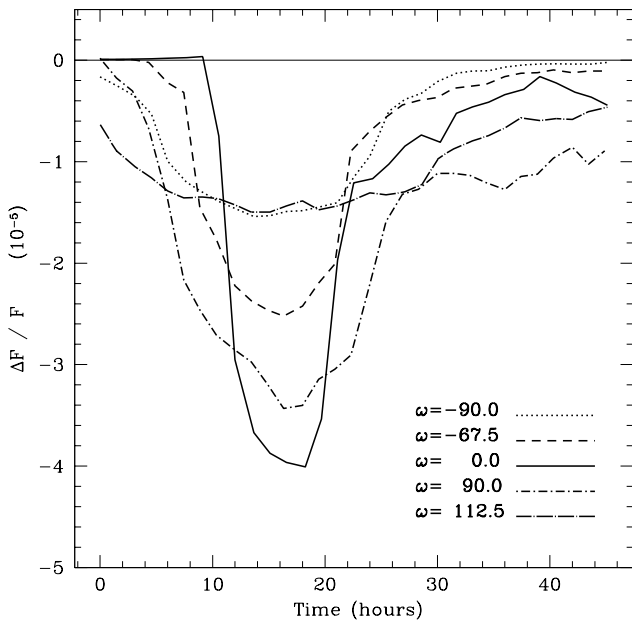
Fig. 4. Same as previous figures. Here the periastron is at 1 AU from a central G type star. The longitude of the periastron ω varies from $-90°$ to $112.5°$ from the line of sight. When $\omega \sim -90°$, the cometary tail is aligned with the line of sight, the light curve presents a more symmetrical shape resembling a planetary occultation

The Cols. 6 to 8 give the fraction of the stellar light scattered by the dust at the same wavelengths. An example of such a table is given in Table 3. A resulting light curve is simply obtained by the addition of the extinction to the scattering at the corresponding wavelength.

3.3. Examples

To illustrate the effect of the parameters, we take as an example the light curve corresponding to the model "50_G_50_10_00_00" and we vary one of the parameters. The resulting light curves are plotted in Figs. 2 to 6. We see that, at a first order, the amplitude of the variation is proportional to the dust production rate and inversely proportional to luminosity/mass ratio.

4. Asymmetry and planet occultation

We can now confirm that the majority of cometary occultations gives light curves with a very particular "rounded triangular" shape (LVF 99 and Fig. 2). As described in LVF 99, this is simply explained by the occultation by the dense cometary head, then followed by the tail which gives only a smaller long lasting additional occultation.

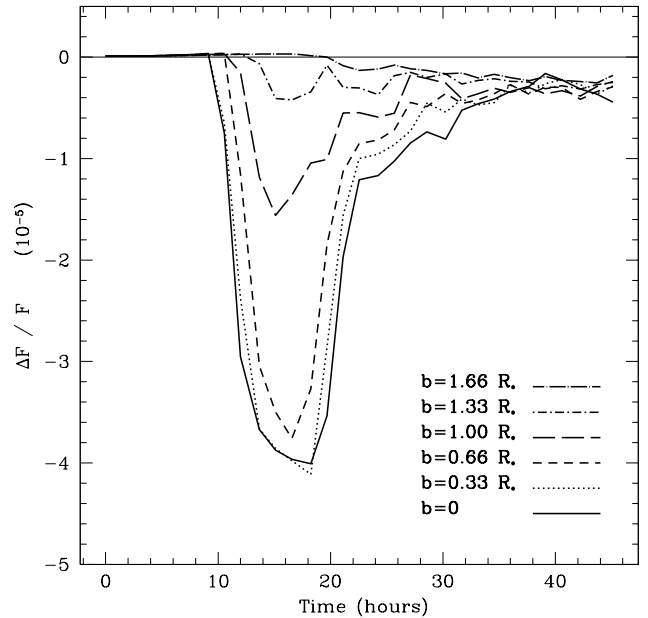However, in some configurations, the tail can be aligned with the line of sight. In these cases the light

Fig. 5. Same as previous figures. Here the impact parameter varies up to 1.66 times the stellar radius
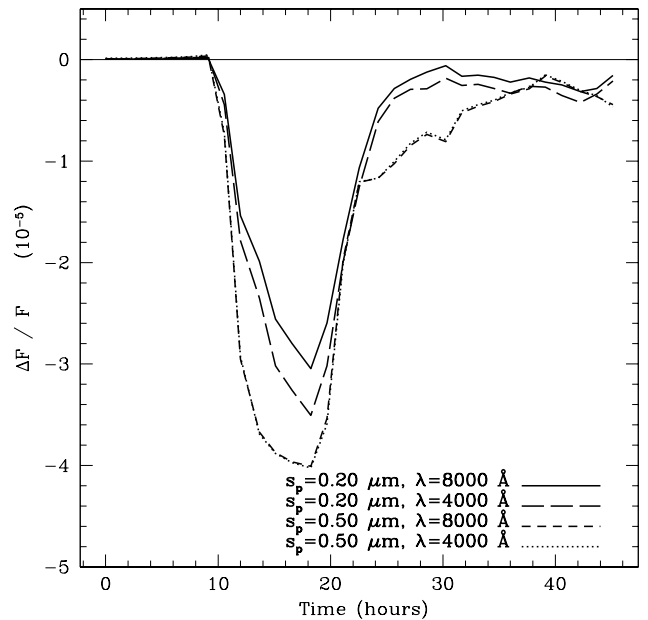

Fig. 6. Same as previous figures. Here we have plotted the light curves in the red and in the blue for the two dust size distributions so-called "20" ($s_{\rm p} = 0.20~\mu$m) and "50" ($s_{\rm p} = 0.50~\mu$m). In the later case, the distribution contains more large dust grains; there is almost no color signature. In the former case with more smaller grains, the extinction is larger at shorter wavelength by about 15%
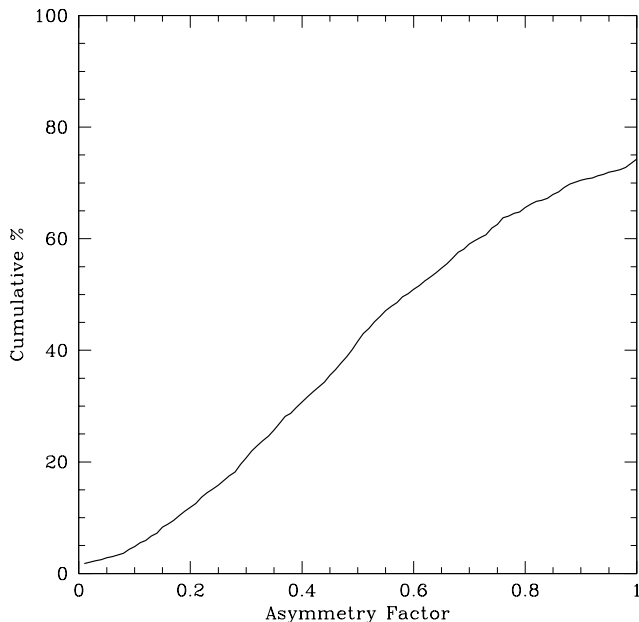
Fig. 7. Plot of the weighted cumulative percentage of light curves with an asymmetry factor smaller than a given value. The asymmetry factor is defined in Sect. 4. Each light curve is given a weight as a function of the periastron q, the production rate P_0 and the type of the central star. We use $dn(q) = q^{0.3}dq$ and $dn(P_0) = P_0^{-2.25}dP_0$ (LVF 99). We consider the proportion of each type of star for a magnitude limited sample of single main sequence stars: K 2%, G 10%, F 31%, A 57%. The maximum percentage does not go up to 100% because the asymmetry factor can be larger than 1. This happens when the scattering dominates the extinction and consequently the star brightness increases, then some points of the photometric variation are significantly positive. We see that the asymmetry factor is smaller than 0.1 for 5% of the light curves, it is smaller than 0.15 in 8% of the cases and smaller than 0.2 in 12% of the cases

curve is more symmetric and can mimic a planetary occultation (Fig. 4, see also Figs. 2 and 3 of LVF 99). Because of the noise, it will be difficult from such observations to differentiate between a comet and a planet.

One of the major difference between a cometary and a planetary occultation is the time-symmetry of the planet occultation light curve. If the photometric variation $V(t) = (\Delta F/F)(t)$ is maximum at $t = t_{\max}$, then for a planet occultation we have $V(t_{\max} - \delta t) = V(t_{\max} + \delta t)$. We can define an "asymmetry factor" by $AF \equiv \mathrm{Max}_{\delta t}|V(t_{\max} - \delta t) - V(t_{\max} + \delta t)|/V(t_{\max})$. Then, for an observation of a planetary occultation with a signal to noise ratio S/N, we have $AF \sim (S/N)^{-1}$, simply because $V(t_{\max} - \delta t)$ and $V(t_{\max} + \delta t)$ are two

noisy measurements of the same value. Thus, cometary occultation light curves can be discriminated if they are asymetric enough with an asymmetry factor larger than a given value defined by the signal to noise ratio of the observation. With the full set of models available, we can evaluate the proportion of cometary occultation symmetric enough to mimic a planetary occultation at a given signal to noise ratio (Fig. 7). As an example, we find that with a signal to noise $S/N \sim 10$, about 5% of cometary occultation light curves can be considered to be symmetric. Following the results of LVF 99, with a survey of 30 000 stars at a photometric accuracy of 10^{-4}, we should be able to detect 100 to 1000 comet occultations per year. This gives about 5 to 50 detections of cometary occultations with symmetric light curves, which could be misinterpreted as planetary occultation. This number is of the same order as the expected number of real planetary occultations by Jupiter-like planets if each star has a planetary system resembling the solar system (LVF 99).

5. Conclusion

It is very likely that in the near future a large number of extra-solar comets will be detected through occultations. We performed a large set of numerical simulations of stars' occultations by extra-solar comets. The result is the apparent photometric variations of the central stars due to these putative comets. We provide here a database of cometary occultation light curves which is electronically available for the preparation of the coming spatial photometric surveys.

As an example, we used this tool to evaluate the number of cometary occultation which present the same symmetrical properties as the planetary occultation. We find that few percents of the comet occultations could be misinterpreted as due to planets.

References

Baglin A., Auvergne M., Barge P., et al., 1997, NASA Origins Conference, Schull M. (eds.)
Biver N., Bockelée-Morvan D., Colom P., et al., 1997, Sci 275, 1915
Hanner M.S., 1983, in Cometary exploration II, Gombosi T.I. (ed.), CRIP Budapest, p. 1
Lecavelier des Etangs A., Vidal-Madjar A., Ferlet R., 1999, A&A 343, 916 (LVF 99)
Newburn R.L., Spinrad H., 1985, AJ 90, 2591
Schleicher D.G., Millis R.L., Birch P.V., 1998, Icarus 132, 397